Daphnia magna filtration efficiency and mobility in laminar to turbulent flows

Teresa Serra*; Aina Barcelona; Marçal Soler and Jordi Colomer

University of Girona. Department of Physics. 17003-Girona

*corresponding author: Teresa.serra@udg.edu

Abstract

Daphnia are filter feeder organisms that prey on small particles suspended in the water column. Since *Daphnia* individuals can feed on wastewater particles, they have been recently proposed as potential organisms for tertiary wastewater treatment. However, analysing the effects of hydrodynamics on *Daphnia* individuals has scarcely been studied. This study focuses then, on quantifying the filtration and swimming velocities of *D. magna* individuals under different hydrodynamic conditions. Both *D. magna* filtration and movement responded differently if the flow was laminar or if it was turbulent. In a laminar-dominated flow regime *Daphnia* filtration was enhanced up to 2.6 times that of a steady flow, but in the turbulent-dominated flow regime *D. magna* filtration was inhibited. In the laminar flow regime *D. magna* individuals moved freely in all directions, whereas in the turbulent flow regime they were driven by the streamlines of the flow. A model based on *Daphnia*-particle encountering revealed that the filtration efficiency in the laminar regime was driven by the length of the *D. magna* individuals and the shear rate imposed by the system.

Introduction

The cladoceran *Daphnia magna* is an organism found in many aquatic systems. It is known to feed on phytoplankton as well as on bacteria, and is responsible for what it is known as the clear water phase of a lake (Burns, 1969; Shiny et al., 2005; Berger et al., 2006; Pau et al., 2013; Lamonica et al., 2016). *Daphnia* individuals can also feed on wastewater particles, which means that a population of *D. magna* can be used as a tertiary treatment to generate water for reuse (Serra et al., 2014). This hypothesis is based on the fact that individuals of *D. magna* provide inactivation levels of 1.4 log units of *E.coli* from wastewater and can reduce turbidity by as much as 60-70% (Serra et al., 2014; Shiny et al., 2005). A population of *D. magna* has also been proved to remove emerging contaminants from wastewater (Garcia-Rodríguez et al., 2014; Matamoros et al., 2012; Matamoros and Bayona, 2013) and to be sensitive to several products, which is why it is a model organism largely used in ecotoxicology (Garreta-Lara et al., 2018).

There are many studies that demonstrate that *Daphnia* individuals reduce their activity when subjected to unfavourable environmental conditions (Gorski and Dodson, 1996; Maceda-Veiga et al., 2015; Chen et al., 2015; Pan et al., 2017). *Daphnia* individuals have been found to exhibit disorders in filter feeding activity, swimming speeds and trajectories, growth, heartbeat, metabolism and survival when exposed to unfavourable factors (Bownik, 2017; Garreta-Lara et al., 2018). Individual unfavourable factors are: high and low temperatures (Berger et al., 2006; Schalau et al., 2008; Serra et al., 2014), high salinities (Bezirci et al., 2012; Liu and Steiner, 2017), high concentrations of chemicals and pharmaceuticals (Pan et al., 2017; Santojanni et al., 2003) and the presence of microplastics (Rehse et al., 2016). A combination of factors such as salinity, temperature and hypoxia has also been proved to negatively affect *D. magna* individuals (Garreta-Lara et al., 2018). For example, temperatures above 26°C coupled with nitrate concentrations above 250 mgL^{-1} produced a 60% mortality in a population of *D. magna*

(Maceda-Veiga et al., 2015). The presence of nitrite increased the mortality of *D. obtusa*, delayed the time to the first batch of eggs and reduced the number of moulting and clutches, especially for nitrite concentrations above 2 mg L^{-1} (Xiang et al., 2012). A change in temperature from 5°C to 25°C induced *D. pulex* individuals to modify trails and sedimentary velocity, and the decrease in the settling velocity was also attributed to the increase in temperature (Gorski and Dodson, 1996). An increase in water temperature from 12°C to 22°C resulted in an increase in the swimming speed of *D. pulex* individuals, thus making them more vulnerable to predators (vulnerability increases from 83% to 121%) as a result of the higher encountering rates between predator and prey (Riessen, 2015). Therefore, the analysis of abiotic parameters in controlled conditions is considered a systematic approach to evaluating *D. magna* performance in stressful environments.

Despite all the studies on how individual factors or combinations of them affect *D. magna* performance, how the flow environment affects their filtration rate is hardly known and is a crucial element when determining the flow rate in any reactor designed to treat water based on *D. magna* filtration. Hydrodynamics might impose some limitations to the normal functioning of Cladocera. An increase in *Daphnia* swimming speed along more tortuous paths, resulting from the chaotic movement of the flow, occurred after turbulence was increased using an oscillating grid (Seuront et al., 2004). The increase in the flow rate due to a reduction in the hydraulic residence time in a wastewater treatment system, impacted the capacity of *D. magna* filtration (Serra and Colomer, 2016). Residence times of 3 h produced high flow velocities and diminished the filtration efficiencies of *D. magna* individuals to 2%, while residence times over 12 h, corresponding to lower flow velocities, increased the filtration efficiencies by over 30%.

In this study, we analyse the behaviour of *D. magna* in a set of experiments encompassing both laminar and turbulent hydrodynamics. The hydrodynamics were generated with a Couette flow system. A Couette flow device is a system composed of two concentric cylinders. When these cylinders rotate, they produce a shear flow in the space between the cylinders, which is a well-known function of their rotating velocities. A Couette flow device also enables a steady controlled flow to be produced (Shimeta et al., 1995) that could encompass a gradual transition from laminar to turbulent conditions (Serra et al., 1997, 2008). This system has been proved to be useful for a number of hydrodynamic purposes such as aggregating and breaking up particles (Serra et al., 1997; Zhu et al., 2016) or studying the influence turbulence has on protozoa feeding (Shimeta et al., 1995).

A total of 34 runs were designed to determine the favourable hydrodynamic flow environment for *D. magna* performance. Filtration capacity and swimming speed are non-intrusive methods and were used as the main parameters to study the responses of *D. magna* individuals to the hydrodynamics of the flow. *Daphnia* swimming behaviour is one of the most sensitive biomarkers in toxicity experiments (Bownik, 2017), while filtration capacity is an indicator of the performance of *D. magna* individuals under variable factors such as water temperature and food availability (Pau et al., 2013; Serra et al., 2014).

Materials and Methods

Couette flow

The flow field was generated by a Couette flow device entailing two concentric cylinders (Figure 1). The inner cylinder had a radius of r_1=2.5 cm and the radius of the outer cylinder was r_2=4.5 cm, i.e. the gap (r_2-r_1) was 2 cm wide. The height of the cylinders was h=15.5 cm. The outer cylinder rotated at an angular velocity that ranged from ω_2=0 rad s^{-1} to 7.39 rad s^{-1} (see Table 1) and the inner cylinder remained at rest (ω_1=0 rad s^{-1}). The space between cylinders was filled up to h_w=13.64 cm. Therefore, the volume of water within the cylinders was 600 ml. The flow velocity in a Couette flow device can be calculated according to Kundu and Cohen (2002),

$$v = ar + \frac{b}{r} \tag{1}$$

where a and b are coefficients that depend on both the radius and the angular velocity of the cylinders and r is any position along the radial axis situated within the gap between cylinders, i.e.

$$a = \frac{\omega_1 r_1^2 - \omega_2 r_2^2}{r_1^2 - r_2^2} \text{ and } b = \frac{\omega_2 r_1^2 r_2^2}{r_1^2 - r_2^2} \tag{2}$$

The mean flow velocity in the Couette system was calculated as

$$\langle v_{Couette} \rangle = \frac{1}{r_2 - r_1} \int_{r_1}^{r_2} v \, dr = \frac{1}{r_2 - r_1} \left[\frac{a}{2} (r_2^2 - r_1^2) + b ln \left(\frac{r_2}{r_1} \right) \right] \tag{3}$$

producing mean velocities in the range of 0 to 17.78 cm s^{-1} (Table 1). The mean shear rate in the flow between cylinders was calculated following Serra et al. (1997),

$$G = \frac{2 \omega r_1 r_2}{r_2^2 - r_1^2} \tag{4}$$

producing shear rates in the range of 0 to 11.87 s^{-1} (Table 1). The Reynolds number for each experimental condition was calculated by

$$Re = \frac{\omega r_2 (r_2 - r_1)}{\nu} \quad (5)$$

where $\nu = 10^{-6}$ m^2 s^{-1} is the kinematic viscosity of the flow. Re ranged from 0 to 6651 (Table 1). As pointed out by Hinze (1975), the transition from a laminar to turbulent flow regime was experimentally found to happen at Re=1900. Therefore, the laminar-dominated regime was characteristic for the runs 1 to 11 (experiments with *D. magna* individuals) and runs 18 to 28 (experiments without *D. magna* individuals), whereas the turbulent-dominated regime was characteristic for runs 12 to 17 (experiments with *D. magna* individuals) and for runs 29 to 34 (experiments without individuals of *D. magna*) (Table 1).

The dissipation rate can be calculated as

$$\varepsilon = G^2 \nu \quad (6),$$

where $\nu = 10^{-6}$ cm^2 s^{-1} is the kinematic viscosity of water (Kundu and Cohen, 2002). In the present study, dissipation ranged from 3.2×10^{-8} to 1.4×10^{-4} m^2 s^{-3} (Table 1), which is within the dissipation range found in natural aquatic systems (Peters and Marrasé, 2000; Peters and Redondo, 1997).

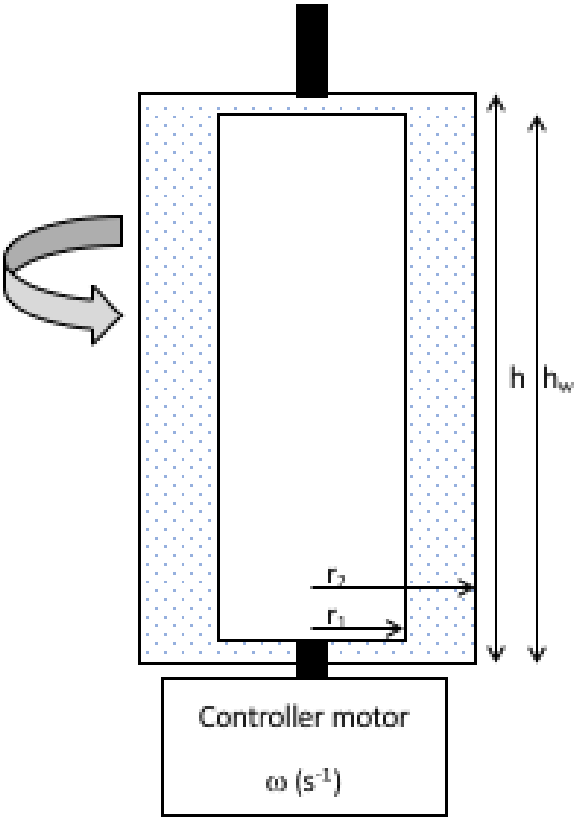

Figure 1. Scheme of the experimental set-up of the Couette flow device. r_1 is the radius of the inner cylinder, r_2 is the radius of the outer cylinder, r_2-r_1 is the gap width between cylinders, h is the height of the outer cylinder and h_w is the water height. ω is the angular velocity of the outer cylinder.

Table 1. Information related to the experimental conditions considered in each run. ω is the angular velocity of the outer cylinder, Re is the Reynolds number of the flow in the gap, $\langle v_{Couette} \rangle$ is the mean velocity in the gap between cylinders calculated from Equation (3), G is the mean shear rate in the gap between cylinders, ε is the dissipation rate calculated from Equation (6) and the flow regime (laminar or turbulent). $C_{Dph+Sed}$

and C_{Sed} correspond to the control experiments with and without *D. magna* individuals, respectively. Dph means *Daphnia*.

		ω (rad s^{-1})	Re	$\langle v_{Couette} \rangle$ (cm s^{-1})	G (s^{-1})	ε (m^2 s^{-3})	Flow Regime
Controls							
With Dph	Without Dph	0	0	0	0	0	Quiescent
$C_{Dph+Sed}$	C_{Sed}						
Runs							
With Dph	Without Dph						
1	**18**	0.11	99	0.26	0.18	3.2×10^{-8}	Laminar flow regime
2	**19**	0.22	198	0.53	0.35	1.2×10^{-7}	
3	**20**	0.39	351	0.94	0.63	3.9×10^{-7}	
4	**21**	0.56	504	1.35	0.90	8.1×10^{-7}	
5	**22**	0.70	630	1.69	1.13	1.3×10^{-6}	
6	**23**	0.83	747	1.99	1.33	1.8×10^{-6}	
7	**24**	1.02	918	2.45	1.64	2.7×10^{-6}	
8	**25**	1.21	1089	2.91	1.94	3.9×10^{-6}	
9	**26**	1.30	1170	3.13	2.09	4.4×10^{-6}	
10	**27**	1.41	1269	3.39	2.27	5.2×10^{-6}	
11	**28**	1.96	1764	4.71	3.15	9.9×10^{-6}	
12	**29**	2.90	2610	6.97	4.66	2.2×10^{-5}	Turbulent flow regime
13	**30**	3.92	3528	9.43	6.30	4.0×10^{-5}	
14	**31**	5.40	4860	12.99	8.68	7.5×10^{-5}	
15	**32**	5.60	5040	13.47	9.00	8.1×10^{-5}	
16	**33**	6.54	5886	15.77	10.51	1.1×10^{-4}	
17	**34**	7.39	6651	17.78	11.87	1.4×10^{-4}	

D. magna characteristics

D. magna individuals were obtained from a laboratory culture maintained for one year at the University of Girona in a 40 L container at 20±1°C and natural daylight photoperiod. A gentle air supply kept the water container oxygenated. The *D. magna* population in the container were fed twice a week with a mixture of commercial spirulina powder and baker's yeast (*Saccharomyces cerevisiae*). Thirty percent of the water from the container was renewed once every fifteen days.

For each experiment, *D. magna* individuals were collected from the container using a mesh with 1 mm spacing to be able to discard individuals smaller than 1 mm long. Individuals retained in the mesh longer than 2 mm were also discarded and returned to the container. Therefore, only 1-2 mm long *D. magna* individuals were considered. Using ImageJ software, the mean size of the *D. magna* individuals was analysed from a video recording of 25 individuals and was found to be 1.6$\pm$0.3 mm. Therefore, the ratio between the width of the gap between the cylinders (2 cm) and the mean length of the *D. magna* individuals (0.16 cm) was 12.5, thus giving *D. magna* individuals enough space to move without interference from the walls (Shimeta et al., 1995).

Experimental method

Each experiment was carried out in a Couette cylinder that was filled with 600 ml of bottled mineral water and 30 ml of spirulina suspension. The spirulina suspension was prepared by diluting 1 g of spirulina powder in 1 L of bottled mineral water, mixed for 30 s at 120 rpm, and left for 1 h so that large spirulina particles would settle. The supernatant was used as the spirulina suspension for the experiments. After introducing the spirulina suspension into the cylinder, 30 *D. magna* individuals were collected from the laboratory culture and gently introduced into the experiments obtaining a final *D. magna* concentration of 50 individuals L^{-1} (hereafter ind L^{-1}).

Control experiments

Two control experiments were carried out under steady flow conditions (ω=0 rad s^{-1}), one with *D. magna* individuals, hereafter $C_{Dph+Sed}$ (Table 1) and another without *D. magna* individuals, hereafter C_{Sed} (Table 1). $C_{Dph+Sed}$ was to assess particle removal by sedimentation as well as *D. magna* filtering abilities in quiescent flow conditions. C_{Sed} provided information on particle removal by both sedimentation in the Couette flow and *D. magna* filtration. To determine $C_{Dph+Sed}$, seventeen experiments with *D. magna* individuals in quiescent water were carried out. The mean on the 17 experiments was considered as the representative result for the control experiment $C_{Dph+Sed}$. To determine C_{Sed}, seventeen experiments were carried out without *D. magna* individuals in quiescent water. The mean of the 17 experiments was considered representative for the control experiment C_{Sed} (Table 1).

D. magna filtration capacity

The spirulina particle size distribution in the suspension was measured with the Lisst-100x particle size analyser (Sequoia Inc.). Samples from each Couette cylinder were taken at different times and analysed to determine the time evolution in the suspended particle concentration. The Lisst 100x consists of a laser beam and an array of detector rings of progressive diameters that allow the light received at the scattering angles of the beam to be analysed. The device measures the particle volume concentration of particles for 32 size-classes, logarithmically distributed in the size range of 2.5-500 μm, using a procedure based on the diffraction theory of light. The Lisst-100x has been found to show good performance in determining particle size distribution and concentration for both organic (Serra et al., 2001) and inorganic particles (Serra et al., 2002a, 2002b) in water suspension. The particle concentration in a desired particle size range was calculated by integrating the concentration of the particles within the range. Since *D. magna* individuals feed on particles less than 30 μm in diameter, the volume concentration of particles within the range of 2.5 to 30 μm was calculated and used as a proxy to evaluate particle removal. It is known that Cladocera ingest organic particles when their size overlaps with the sizes of the organic particles they feed on (Arruda et al., 1983; Gliwicz, 1990).

Since the temporal evolution of the suspended particle concentration decreased exponentially, the concentration may be described by an exponential decay equation as follows (Pau et al., 2013):

$$c = c_0 e^{-kt} \tag{7}$$

where k is the rate of particle removal by both sedimentation (k_s) and *D. magna* filtration (k_{Dph}), i.e. $k=k_s+k_{Dph}$.

From Equation (7) k can be solved following

$$k = -\frac{1}{t} ln\left(\frac{c}{c_0}\right) \tag{8}$$

and k_s can be determined from those experiments without individuals of *D. magna* (in which $k_{Dph}=0$). Therefore, k_{Dph} will be calculated for the rest of the experiments. The rate of decrease due to *D. magna* filtration is a function of the filtering rate of each *D. magna* individual (F, in ml ind^{-1} L^{-1}) and the *D. magna* concentration in such a way that (Pau et al., 2013),

$$k_{Dph}=F\times C_{Dph} \quad (9).$$

D. magna filtration versus the shear rate

The kinetics of particle collision and coagulation in a system of two populations in a sheared flow has been formulated by Li and Logan (1997). In this study, the two populations are *D. magna* and small suspended particles. The rate of small particles captured by a single *D. magna* individual R_{Dph} can be written as

$$R_{Dph} = \alpha G L^3 c + R(0) \quad (10),$$

where α is the capture efficiency for each *D. magna* individual, G is the shear rate, L is the *D. magna individuals* length-scale and $R(0)=k_{Dph}(0)\times c$ is the particle removal by each *D. magna* individual in a steady flow (i.e. at $G=0\ s^{-1}$). Therefore, the rate of the decrease of small suspended particles due to *D. magna* feeding can be written as

$$\frac{1}{c_{Dph}}\frac{dc}{dt} = -\alpha G L^3 c - \frac{R(0)}{c_{Dph}} \quad (11)$$

and merging Equation (7) and Equation (11) results in

$$-\frac{c_0}{c_{Dph}} k_{Dph}(G) e^{-k_{Dph}(G)t} = -\alpha G L^3 c - \frac{k_{Dph}(0)c}{c_{Dph}} \quad (12)$$

and with Equation (7)

$$\frac{k_{Dph}(G)}{c_{Dph}} = \alpha G L^3 + \frac{k_{Dph}(0)}{c_{Dph}} \quad (13)$$

and therefore

$$k_{Dph}(G) = \alpha c_{Dph} G L^3 + k_{Dph}(0) \quad (14).$$

Using Equations (9) and (14) the filtration F is a function of G, α and L, that can be written as

$$F = \alpha G L^3 + F(0) \quad (15).$$

where $F(0)=k_{Dph}(0)/c_{Dph}$.

D. magna trails and *D. magna* speed

The analysis of *D. magna* velocity was carried out by videotaping the movement of the *D. magna* individuals. The camera recorded 25 frames per second and the *D. magna* trails were recorded for 1 minute for each case, giving a total of 1,500 frames. These frames were analysed with ImageJ software using the mTrack plug-in following Maison et al. (2012) and Pan et al. (2017). At each time step the positions in the x (horizontal) and y (vertical) axis were analysed and the velocities in the x and y directions calculated. Ten *D. magna* individuals were considered in each case and a mean value for the velocities was calculated. A scheme of the trail followed by one representative *D. magna* individual is presented in Figure 2. The x and y component of the velocity is represented and calculated from the temporal evolution of the (x,y) positions of each *D. magna* individual at each time step. The ratio v_y/v_x was calculated afterwards. The lengths of the trajectories considered for the analysis were between 6 and 7 cm. Therefore, the mean *D. magna* speed was calculated as

$$v_{Dph} = \sqrt{\left(\overline{v_x}^2 + \overline{v_y}^2\right)} \quad (16)$$

where v_x and v_y are the mean velocities of all the trails in the x and y axis, respectively.

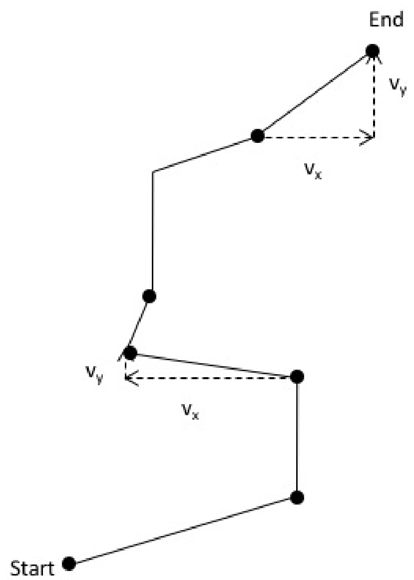

Figure 2. Scheme of a *D. magna* trail from the start to end points considered. The vertical (v_y) and horizontal velocities (v_x) are included in the schematics.

Results

D. magna swimming velocity

The average speed of *D. magna* individuals when the flow was at rest, corresponding to the control $C_{Dph+Sed}$, was calculated from v_x and v_y following Equation (16) and was found to be 7±2 cm s^{-1} for a mean *D. magna* body length of 1.6 mm (Figure 3). When considering the margin of error, this speed is on the scale of that obtained from the empirical allometric equation (Kunze, 2011; Wickramarathna et al., 2014) for cruising velocity versus *D. magna* body length $u_c=3.23L^{0.83}=11.1$ cm s^{-1}. Therefore, this result indicates that the movement of *D.* magna individuals was not affected by the vertical and horizontal constraints of the experiment.

The ratio v_y/v_x versus the mean flow velocity in the Couette was calculated and plotted (Figure 3). The ratio v_y/v_x was 2 for the experiments carried with the fluid at rest. As the mean Couette flow velocity increased, the ratio v_y/v_x decreased sharply, reaching a value of 0.2 at 3 cm s^{-1} and nearly 0 at 7 cm s^{-1}. For velocities over 7 cm s^{-1}, *D. magna* trails were mainly in the x direction following the direction of the fluid and no movement along y was observed. In addition, observing the video recording, *D. magna* individuals tended to move against the flow under slow Couette flow velocities, whereas at high Couette flow velocities they moved with the flow direction. That is, as the Couette flow velocity increased it provided a greater velocity in the x-axis, thus reducing the ability of *D. magna* individuals to swim in the vertical direction. In all the experiments, the vertical distribution of *D. magna* was homogeneous along the working height in the Couette flow.

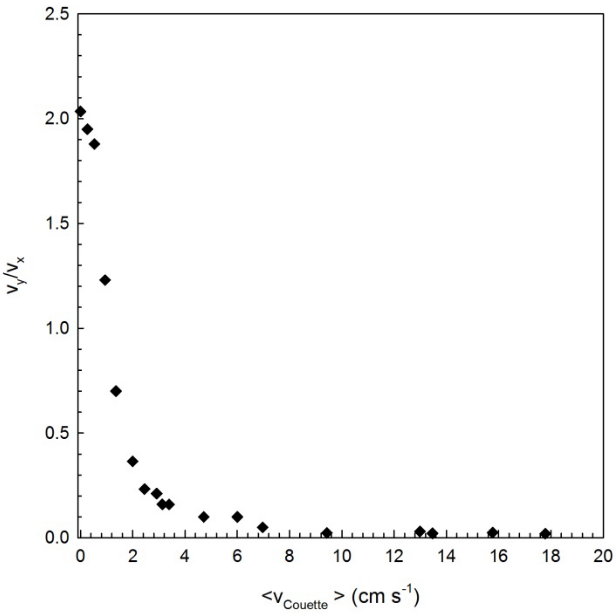

Figure 3. Ratio v_y/v_x versus the mean Couette flow velocity ($\langle v_{Couette} \rangle$, in cm s^{-1}).

Instantaneous speeds of *D. magna* individuals (Equation 16) were averaged over time and plotted versus the mean Couette flow velocity (Figure 4). For mean Couette flow velocities below 3 cm s^{-1}, *D. magna* swimming speeds increased following a non-linear trend, but remained higher than the Couette velocity. For flow velocities above 7 cm s^{-1}, *D. magna* speeds followed a linear (1:1) relationship with the mean flow velocity in the Couette system, indicating the inability of *D. magna* individuals to swim freely and demonstrating that *D. magna* individuals were being forced to follow the streamlines of the flow. The change in the dynamics of the *D. magna* velocities coincided with the change in the hydrodynamics of the flow regime. For Couette flow velocities below 7 cm s^{-1}, the flow regime was laminar with Re=1746, while for higher Re the flow was turbulent.

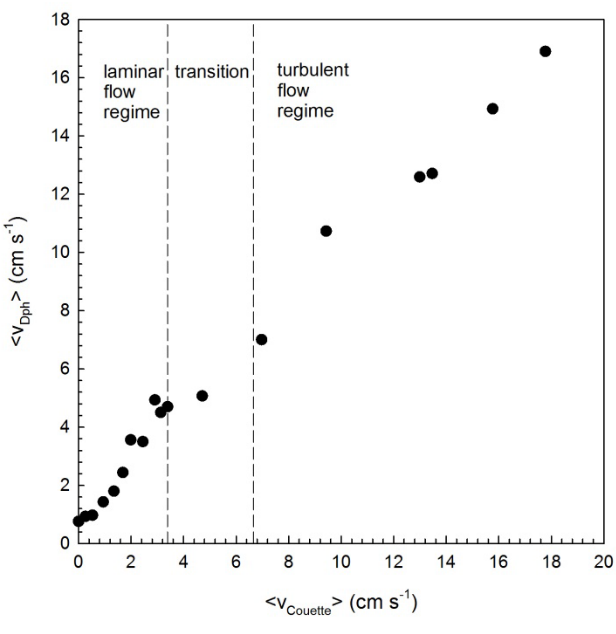

Figure 4. Mean speed of *D. magna* individuals ($<v_{Dph}>$ in cm s^{-1}, calculated with Equation (16)) plotted versus the mean Couette flow velocity ($<v_{Couette}>$, in cm s^{-1}). Vertical dashed lines correspond to the different Couette flow regimes (Table 1).

Temporal evolution of the particle removal

In Figure 5a the particle volume concentration of the suspension with spirulina for the range of measured particles in the control experiment $C_{Dph+Sed}$ (conducted at rest, Table 1) with *D. magna* individuals is presented at t=0 h and at t=5 h. A decrease in the particle volume concentration with time is observed. The decrease in the suspended particle concentration of particles with diameters below 30 μm was caused by both the capacity of *D. magna* individuals to filter as well as particle sedimentation.

The time evolution of the particle ratio of the concentration to the initial particle concentration (at t=0h) was also calculated for the control experiments $C_{Dph+Sed}$ and C_{Sed} and plotted in Figure 5b. The temporal evolution of c/c_0 with time for both control experiments shows that the decrease in particle concentration in the case without *D. magna* was slower than that for the case with *D. magna* due to the extra feeding on the suspended particles by *D. magna* individuals. Since the decrease in the particle concentration is expected to be exponential (Pau et al., 2013; Serra and Colomer, 2016) the characteristic time t at which c/c_0 decreased in e^{-1}=0.37 was considered as the characteristic time in all the experiments. This time was approximately 4 h of treatment. Therefore, c/c_0 at t=0h and at t=4h were considered in the calculations for all the experiments.

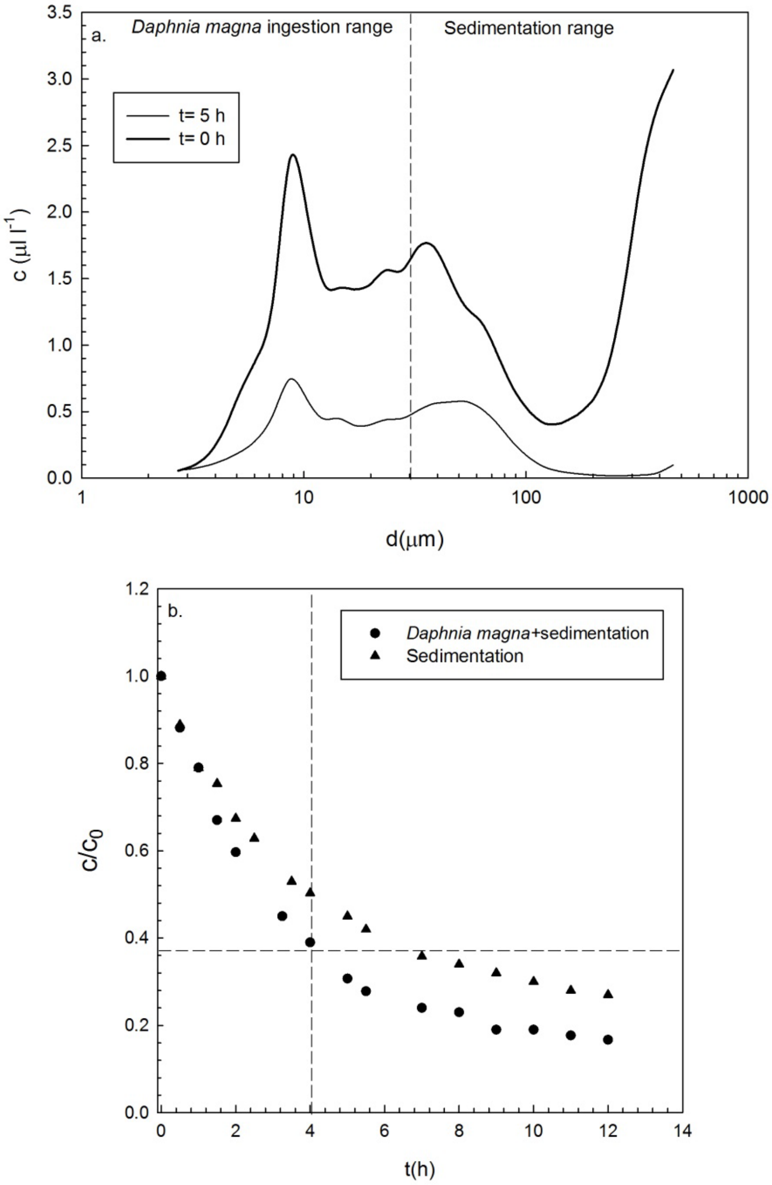

Figure 5. (a) Particle size distribution for the case of control experiment $C_{Dph+Sed}$ carried out at rest (ω=0 s^{-1}) for two time steps, initially (t=0h) and after 5h of treatment (t=5h). The dashed vertical line corresponds to the limit of the ingestion particle size by *D. magna* individuals. In the vertical axis, the particle volume concentration in μl L^{-1} is represented and in the x-axis the diameter of the suspended particles in μm. **(b)** Temporal evolution of the ratio c/c_0 for the two control experiments ($C_{Dph+Sed}$ and C_{Sed}).

Vertical and horizontal lines determine the time when the ratio c/c_0 was reduced to $1/e=0.37$ (corresponding to a $t=4$h of treatment).

The ratio of c/c_0, calculated for control experiments ($C_{Dph+Sed}$ and C_{Sed}), runs 1-17 (with *D. magna* individuals) and runs 18-34 (without *D. magna* individuals) versus the mean Couette flow velocity, calculated by Equation (3) is presented in Figure 6. For the experiments without individuals of *D. magna*, c/c_0 was nearly 0.55 at rest ($\langle v_{Couette} \rangle=0$ cm s^{-1}) and remained constant up to a mean Couette flow velocity of 7 cm s^{-1}, increasing slightly afterwards up to 0.58 for a Couette velocity of 18 cm s^{-1}. For the experiments with individuals of *D. magna,* c/c_0 was 0.45 at rest, decreasing to a minimum of 0.33 for a Couette velocity of 3 cm s^{-1}. For mean Couette flow velocities above 3 cm s^{-1}, c/c_0 sharply increased up to 0.55 for $\langle v_{Couette} \rangle=7$ cm s^{-1}. For mean Couette velocities above 7 cm s^{-1}, c/c_0 was the same as that obtained for the runs without *D. magna* individuals. The decrease in c/c_0 coincided with the conditions dominated by the laminar flow regime, while the turbulent flow regime coincided with c/c_0 values above those at steady flow conditions and equal to those obtained without *D. magna* individuals.

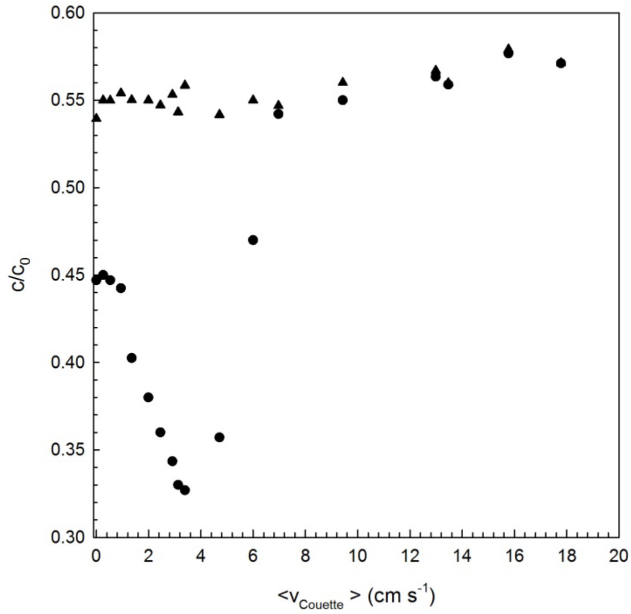

Figure 6. Ratio of the particle volume concentration (c/c_0) versus the mean Couette flow velocity ($<v_{Couette}>$, in cm s^{-1}) for the runs with and without *D. magna* individuals.

D. magna filtration capacity

The filtration capacity (F) of *D. magna* for each experiment in the Couette flow was calculated with Equations (8) and (9) and plotted in Figure 7. The filtration capacity at rest was 1 ml ind^{-1} h^{-1} and increased up to 2.6 ml ind^{-1} h^{-1} in the laminar flow regime. In the transition from laminar to turbulent flow regimes, the filtration capacity dropped down to 1 ml ind^{-1} h^{-1}, i.e. attaining the same filtration like that in a quiescent flow. Higher flow velocities observed in the turbulent regime inhibited *D. magna* filtration capacity and, as a result, filtration remained nearly constant and equal to 0 ml ind^{-1} h^{-1}.

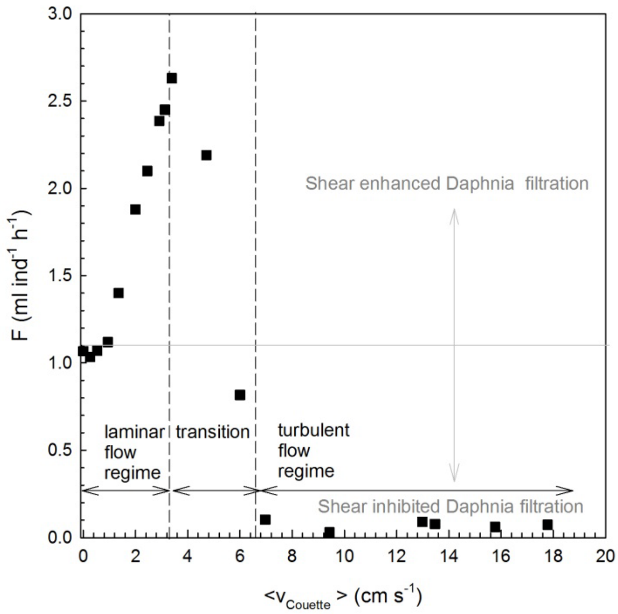

Figure 7. Filtration capacity of *D. magna* individuals (in ml ind^{-1} h^{-1}) versus the mean Couette flow velocity ($<v_{Couette}>$, in cm s^{-1}). Vertical dashed lines correspond to the different Couette flow regimes (Table 1). The horizontal line corresponds to the *D. magna* filtration in quiescent flow.

Discussion

The hydrodynamic flow regime is a crucial parameter in determining the performance of *D. magna* because it modifies both the filtering capacity and the mobility of *D. magna* individuals. The laminar dominated flow regime enhanced the filtration efficiency by *D. magna* individuals, whereas the turbulent flow regime produced an inhibitory effect on *D. magna* filtration.

The filtration capacity of 1.6 mm long *D. magna* individuals in quiescent flow conditions was 1 ml ind^{-1} h^{-1}, which is close to that found by Burns (1969) for the same body length and at a water temperature of 20° C. The increase in the filtration capacity obtained here when *D. magna* individuals are under a mean flow, is attributed to the increase in the particle-*Daphnia* encountering frequency, enhancing the rate of particle removal by *D. magna* filtering. However, this positive effect was only found in the laminar flow regime. In the transition, F sharply decreased with a further increase in the Couette flow velocity. In the turbulent regime, F reached a minimum value of nearly 0 ml ind^{-1} h^{-1}, which remained constant thereafter, inhibiting the filtration capacity of *D. magna* individuals. The decrease in the *D. magna* filtration efficiency coincides with the transition from the laminar to turbulent flow conditions that would be expected to hold for Re=1900 (Hinze, 1975). For high Couette flow velocities, *D. magna* were unable to filtrate, thus the flow regime supressed the feeding. This might be attributed to the fact that the time available for a *D. magna* individual to complete the capture of an encountered particle is less than that required to be ingested successfully (Lewis and Pedley, 2001; MacKenzie et al., 1994). As pointed out by MacKenzie et al., (1994), the encounter between a predator and its prey is a necessary but not sufficient condition for ingestion. The fact that ingestion rates are maximal at low flow velocities, corresponding to the laminar flow regime, responds to the fact that while encounters increase with turbulence, successful capture of prey by predators decreases with turbulence.

The change in the filtration capacity of *D. magna* with the increase in flow velocity is in accordance with the change in their swimming trajectories. For mean Couette flow velocities in the turbulent regime, *D. magna* individuals were unable to swim freely in both directions (x and y) and their trajectories were completely determined by the flow streamlines along x. This fact may impose a limit on the correct functioning of *D. magna* individuals, in terms of their feeding capacity, when the flow velocity dominates over the *D. magna* swimming speed. Bownik (2017) indicated that alterations in *D. magna* trajectories may suggest disorders in the *D. magna* nervous system manifested through a loss of orientation.

In the laminar flow regime, *D. magna* speeds were above the mean Couette flow velocity. However, in the turbulent flow regime *D. magna* individuals could not overcome the velocity of the flow and they were forced to travel in the same direction as the fluid. *D. magna* movement in quiescent flow produced viscous dissipation rates of 3.4×10^{-6} m^2 s^{-3} for 2 mm long *D. magna* individuals (Wickramarathna et al., 2014). In the present study, dissipation coincides with the dissipation for the transition from the laminar to turbulent flow (Table 1). Therefore, both the swimming speed and the trails of *D. magna* might be modified when the dissipation produced by the flow overpowers the dissipation produced by the movement of *D. magna* individuals.

Burns (1969) pointed out that the filtration rate of *D. magna* individuals increases with body length with a power dependence, where the power (that ranged from 2.16 to 2.80) is a function of the water temperature (that ranged from 15 °C to 25 °C). Burns found the maximum power dependence to be 2.80 when the temperature was 20 °C. It must be noted that the model proposed here for F with the *D. magna* length L, has a power relationship of 3 (Equation 15), which is close to that found experimentally by Burns

(1969). The filtration model has been used to fit the data in this study, taking into consideration the *D. magna* mean diameter (d=1.6 mm) and the filtration obtained in this study in the laminar regime, where the shear rate enhanced *D. magna* filtration. A linear fit between F and G was found for the laminar flow regime ($0<G<2.2\ s^{-1}$) with a slope of 0.82 and a y-axis interception of 0.767 (Figure 8a, r^2=0.9797, 99% of confidence). This resulted in α=0.056 ind^{-1}. Then, according to Equation (15) the *D. magna* filtration can be written as

$$F = 0.056GL^3 + 0.767 \quad (17).$$

Therefore, for the range of G in the laminar-dominated region, F increases linearly with G and to the third power of the *D. magna* length (Figure 8a). From the linear fitting equation F(0)=0.767 ml ind^{-1} h^{-1}.

The result of the model has been used to predict F for four different *D. magna* lengths (1 mm, 1.5 mm, 2 mm and 3 mm). To obtain F(0) for these *D. magna* lengths, i.e. the filtration at steady flow conditions at 20 °C, the experimental results obtained by Burns (1969) were considered (i.e. 0.15 ml ind^{-1} h^{-1}, 0.6 ml ind^{-1} h^{-1}, 2 ml ind^{-1} h^{-1} and 5.5 ml ind^{-1} h^{-1}, respectively). As shown in Figure 8b, for a *D. magna* diameter of d=3 mm, F increases from F~5.5 ml ind^{-1} h^{-1} at G=0 s^{-1} to F~17.7 ml ind^{-1} h^{-1} at G=2.27 s^{-1}. Therefore, for *D. magna* body lengths of d=3 mm, the model predicts a 3.2-fold increase in the *D. magna* filtration when they are under a laminar-dominated flow field. This increase is close to the 3.4-fold increase for *D. magna* individuals of 1.6 mm for the same range of G. The model also predicts an 8-fold increase for F when the *D. magna* length doubles.

This result is relatively close to the 9-fold increase in F at steady flow conditions when *D. magna* length doubles from 1.5 mm to 3 mm (Burns, 1969).

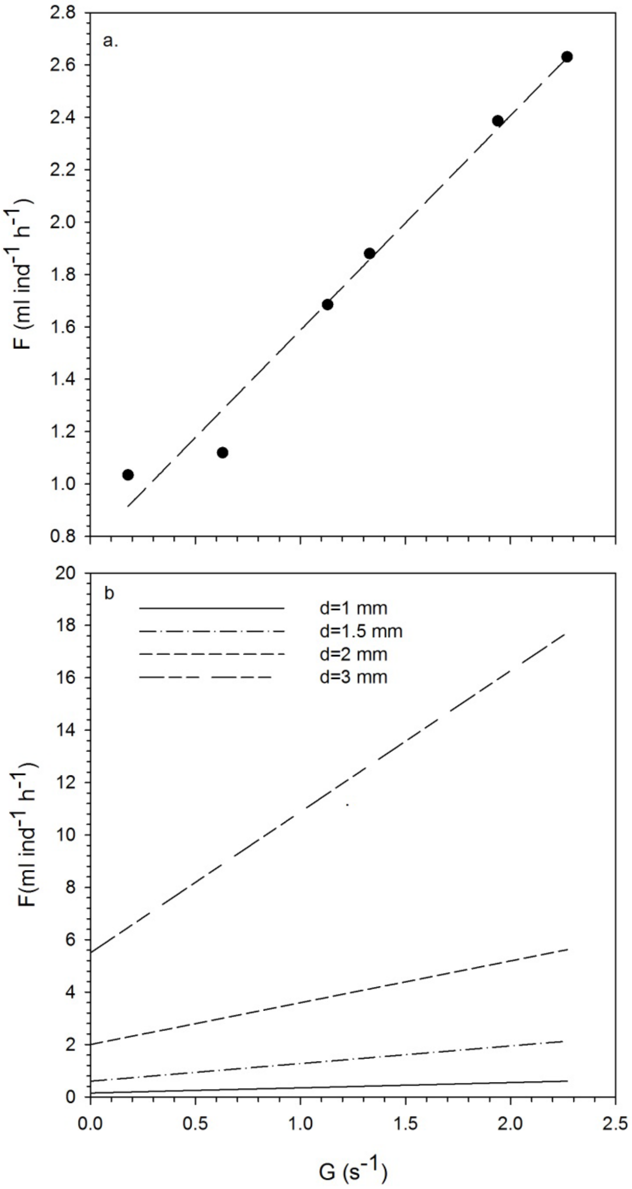

Figure 8. (a) F (in ml ind^{-1} h^{-1}) versus G (in s^{-1}) for the laminar-dominated flow regime. The dashed line represents the linear best fit of the data with an equation F=0.820G+0.767, with r^2=0.9797 and 99% confidence. **(b)** F (in ml ind^{-1} h^{-1}) versus G (in s^{-1}) predicted by the model (Equation (15)) for four different *D. magna* lengths (L=1 mm, 1.5 mm, 2 mm and 3 mm) in the laminar-dominated flow regime.

Conclusions

The trails, swimming velocity and filtration efficiency of *D. magna* were found to depend on the hydrodynamics of the flow. In the laminar flow regime, the shear enhanced filtration and *D. magna* swimming speeds were partially affected by the flow, however, in the turbulent flow regime, the shear inhibited the *D. magna* filtration and *D. magna* trails were forced to follow the flow's streamlines.

In the laminar-dominated flow regime, and for *D. magna* individuals of mean length of 1.6 mm, the maximum *D. magna* filtration rate was 2.6 ml ind^{-1} h^{-1}; 160% greater than that obtained in a quiescent flow. This result indicates that *D. magna* filtration capacity might be enhanced for intermediate flow environments due to the increase in the encountering rate between *D. magna* individuals and suspended particles. However, filtration might be completely supressed at high flow environments because *D. magna* individuals are unable to complete particle capture in such conditions.

These results provide information about how important flow regime is for the filtration capacity of *D. magna* individuals, and indicate the maximum velocities and the appropriate flow regime for obtaining the maximum efficiency for a tertiary treatment reactor based on *D. magna* filtration. Therefore, based on these findings, the residence time within a reactor needs to be carefully considered to satisfy the required flow regime in a reactor based on *D. magna* filtration.

Acknowledgements

This work was supported by the University of Girona funding MPCUdG2016 and by the INNOQUA project from the European Union's Horizon 2020 research and innovation program (Ares(2016)1770486).

References

Arruda, J.A., Marzolf, G.R., Flauk, R.T., 1983. The role of suspended sediments in the nutrition of zooplankton in turbid reservoirs. Ecology 64, 1225–1235.

Berger, S.A., Diehl, S., Stibor, H., Trommer, G., Ruhenstroth, M., Wild, A., Weigert, A., Jäger, C.G., Striebel, M., 2006. Water temperature and mixing depth affect timing and magnitude of events during spring succession of the plankton. Oecologia 150, 643–654. doi:10.1007/s00442-006-0550-9

Bezirci, G., Akkas, S.B., Rinke, K., Yildirim, F., Kalayloiglu, Z., Severcan, F., Beklioglu, M., 2012. Impacts of salinity and fish-exuded kairomone on the survival and macromolecular profile of Daphnia pulex. Ecotoxicology 21, 601–614.

Bownik, A., 2017. Daphnia swimming behaviour as a biomarker in toxicity assessment: A review. Sci. Total Environ. 601–602, 1–1868.

Burns, C., 1969. The relationship between body size of filter-feeding Cladocera and the maximum size of particle ingested. Limnol. Oceanogr. 14, 693–700.

Burns, C.W., 1969. Relation between filtering rate, temperature, and body size in four species of Daphnia. Limnol. Oceanogr. 14, 693–700.

Chen, T., Xu, Y., Zhu, S., Cui, F., 2015. Combining physico-chemical analysis with a Daphnia magna bioassay to evaluate a recycling technology for drinking water treatment plant waste residuals. Ecotoxicol. Environ. Saf. 122, 368–376. doi:10.1016/j.ecoenv.2015.08.023

Garcia-Rodríguez, A., Matamoros, V., Fontàs, C., Salvadó, V., 2014. The ability of biologically based wastewater treatment systems to remove emerging organic contaminants—a review. Environ. Sci. Pollut. Res. 21, 11708–11728. doi:10.1007/s11356-013-2448-5

Garreta-Lara, E., Campos, B., Barata, C., Lacorte, S., Tauler, R., 2018. Combined effects of salinity, temperature and hypoxia on Daphnia magna metabolism. Sci. Total Environ. 610–611, 602–612.

Gliwicz, Z.M., 1990. Food thresholds and body size in Cladocerans. Nature 343, 638–640.

Gorski, P.R., Dodson, S.I., 1996. Free-swimming Daphnia pulex can avoid following Stokes' law. Limnol. Oceanogr. 41, 1815–1821.

Hinze, J.O., 1975. Turbulence. McGraw-Hill.

Kundu, P.K., Cohen, I.M., 2002. Fluid Mechanics. Academic Press, London.

Kunze, E., 2011. Fluid mixing by swimming organisms in the low-Reynolds-number limit. J. Mar. Res. 69, 591–601.

Lamonica, D., Herbach, U., Orias, F., Clément, B., Charles, S., Lopes, C., 2016. Mechanistic modelling of daphnid-algae dynamics within a laboratory microcosm. Ecol. Modell. 320, 213–230.

Lewis, D.M., Pedley, T.J., 2001. The influence of turbulence on plankton predation strategies. J. Theor. Biol. 210, 347–365. doi:10.1006/jtbi.2001.2310

Li, X., Logan, B.E., 1997. Collision frequencies between fractal aggregates and small particles in a turbulently sheared fluid. Environ. Sci. Technol. 31, 1237–1242.

Liu, X., Steiner, C.F., 2017. Ecotoxicology ofsalinity tolerance in Daphnia pulex: interactive effects of clonal variation, salinity stress and predation. J. Plankton Res. 39, 687–697.

Maceda-Veiga, A., Webster, G., Canals, O., Salvadó, H., Weightman, A.J., Cable, J., 2015. Chronic effects of temperature and nitrate pollution on Daphnia magna: Is this cladoceran suitable for widespread use as a tertiary treatment? Water Res. 83, 141–152. doi:10.1016/j.watres.2015.06.036

MacKenzie, B.R., Miller, T.J., Cyr, S., Leggett, W.C., 1994. Evidence for a dome-shaped relationship between turbulence and larval fish ingetion rates. Limnol. Oceanogr. 39, 1790–1799.

Matamoros, V., Bayona, J.M., 2013. Removal of pharmaceutical compounds from wastewater and surface water by natural treatments. Compr. Analyitical Chem. 62, 409–437.

Matamoros, V., Sala, L., Salvadó, V., 2012. Evaluation of a biologically-based filtration water reclamation plant for removing emerging contaminants: A pilot plant study. Bioresour. Technol. 104, 243–249.

Moison, M., Schmitt, F.C., Souissi, S., 2012. Effect of Temperature on Temora longicornis swimming behaviour: Illustration of seasonal effects in a temperate ecosystem. Aquat. Biol. 16, 149–162.

Pan, Y., Yan, S.-W., Li, R.-Z., Hu, Y.-W., Chang, X.-X., 2017. Lethal/sublethal responses of Daphnia magna to acute norfloxacin contamination and changes in phytoplankton-zooplankton interactions induced by this antibiotic. Sci. Rep. 7.

Pau, C., Serra, T., Colomer, J., Casamitjana, X., Sala, L., Kampf, R., 2013. Filtering capacity of Daphnia magna on sludge particles in treated wastewater. Water Res. 47, 181–186. doi:10.1016/j.watres.2012.09.047

Peters, F., Marrasé, C., 2000. Effects of turbulence on plankton: an overview of experimental evidence and some theoreti- cal considerations. Mar. Ecol. Prog. Ser. 205, 291–306.

Peters, F., Redondo, J.M., 1997. Turbulence generation and mea- surement: application to studies on plankton. Sci. Mar. 61, 205–228.

Rehse, S., Kloas, W., Zar, C., 2016. Short-term exposure with high concentrations of pristine microplastic particles leads to immobilisation of Daphnia magna. Chemosphere 153, 91–99. doi:10.1016/j.chemosphere.2016.02.133

Riessen, H.P., 2015. Water temperature alters predation risk and the adaptative landscape of induced defences in plankton communities. Limnol. Oceanogr. 60, 2037–2047.

Santojanni, A., Rossolini, G., Gorbi, G., Piantanelli, L., Sartore, F., 2003. Use of a mathematical model in the analysis of survival curves of Daphnia magna exposed to toxicants. Water Res. 37, 2357–2364.

Schalau, K., Rinke, K., Straile, D., Peters, F., 2008. Temperature is the key factor exdplaining interannual variability of Daphnia development in spring: a modelling study. Glob. Chang. Biol. 157, 531–543.

Serra, T., Colomer, J., 2016. The hydraulic retention time on the particle removal efficiency by Daphnia magna filtration on treated wastewater. Int. J. Environ. Sci. Technol.

Serra, T., Colomer, J., Casamitjana, X., 1997. Aggregation and breakup of particles in a

shear flow. J. Colloid Interface Sci. 187, 466–73. doi:10.1006/jcis.1996.4710
Serra, T., Colomer, J., Cristina, X., Vila, X., Arellano, J.B., Casamitjana, X., 2001. Evaluation of a laser in situ scattering instrument for measuring the concentration of phytoplankton, purple sulphur bacteria and suspended inorganic sediments in lakes. J. Environ. Eng. 127, 1023–1030.
Serra, T., Colomer, J., Gacia, E., Soler, M., Casamitjana, X., 2002a. Effects of a turbid hydrothermal plume on the sedimentation rates in a karstic lake. Geophys. Res. Lett. doi:10.1029/2002GL015368
Serra, T., Colomer, J., Logan, B.E., 2008. Efficiency of different shear devices on flocculation. Water Res. 42, 1113–1121. doi:10.1016/j.watres.2007.08.027
Serra, T., Colomer, J., Pau, C., Marín, M., Sala, L., 2014. Tertiary treatment for wastewater reuse based on the Daphnia magna filtration – Comparison with conventional tertiary treatments. Water Sci. Technol. 70, 705–710. doi:10.2166/wst.2014.284
Serra, T., Colomer, J., Zamora, L., Moreno-Amich, R., Casamitjana, X., 2002b. Seasonal development of a turbid hydrothermal lake plume and the effects on the fish distribution. Water Res. 36, 2753–2760. doi:10.1016/S0043-1354(01)00510-3
Seuront, L., Yamazaki, H., Souissi, S., 2004. Hydrodynamic disturbance and zooplankton swimming behavior. Zool. Stud. 43, 376–387.
Shimeta, J., Jumars, P.A., Lessard, E.J., 1995. Influences of turbulence on suspension feeding by planktonic protozoa; experiments in laminar shear fields. Limnol. Oceanogr. 40, 845–859.
Shiny, K., Remani, K., Nirmala, E., Jalaja, T., Sasidharan, V., 2005. Biotreatment of wastewater using aquatic invertebrates, Daphnia magna and Paramecium

caudatum. Bioresour. Technol. 96, 55–58. doi:10.1016/j.biortech.2004.01.008
Wickramarathna, L.N., Noss, C., Lorke, A., 2014. Hydrodynamic trails produced by Daphnia: size and energetics. PLoS One 9, e92383.
Xiang, F., Geng, L., Lü, K., Zhang, J., Minter, E.J.A., Yang, Z., 2012. Effect of long-term nitrite exposure on the cladoceran Daphnia obtusa: Survival, moults, and reproduction. Biochem. Syst. Ecol. 41, 98–103.
Zhu, Z.., Wang, H.., Yu, J.S., Doug, J., 2016. On the kaolinite floc size at the steady state of flocculation in a turbulent flow. PLoS One 11, e0148895.

Figure Legends

Table 1. Information related to the experimental conditions considered in each run. ω is the angular velocity of the outer cylinder, Re is the Reynolds number of the flow in the gap, $<v_{Couette}>$ is the mean velocity in the gap between cylinders calculated from Equation (3), G is the mean shear rate in the gap between cylinders, ε is the dissipation rate calculated from Equation (6) and the flow regime (laminar or turbulent). $C_{Dph+Sed}$ and C_{Sed} correspond to the control experiments with and without Daphnia individuals, respectively. Dph means *Daphnia*.

Figure 1. Scheme of the experimental set-up of the Couette flow device. r_1 is the radius of the inner cylinder, r_2 is the radius of the outer cylinder, r_2-r_1 is the gap width between cylinders, h is the height of the outer cylinder and h_w is the water height. ω is the angular velocity of the outer cylinder.

Figure 2. Scheme of a *D. magna* trail from the start to end points considered. The vertical (v_y) and horizontal velocities (v_x) are included in the schematics.

Figure 3. Ratio v_y/v_x versus the mean Couette flow velocity ($<v_{Couette}>$, in cm s^{-1}).

Figure 4. Mean speed of *D. magna* individuals ($<v_{Dph}>$ in cm s^{-1}, calculated with Equation (16)) plotted versus the mean Couette flow velocity ($<v_{Couette}>$, in cm s^{-1}). Vertical dashed lines correspond to the different Couette flow regimes (Table 1).

Figure 5. (a) Particle size distribution for the case of control experiment $C_{Dph+Sed}$ carried out at rest (ω=0 s^{-1}) for two time steps, initially (t=0h) and after 5h of treatment (t=5h). The dashed vertical line corresponds to the limit of the ingestion particle size by *D. magna* individuals. In the vertical axis, the particle volume concentration in μl L^{-1} is represented and in the x-axis the diameter of the suspended particles in μm. **(b)** Temporal evolution of the ratio c/c_0 for the two control experiments ($C_{Dph+Sed}$ and C_{Sed}).

Vertical and horizontal lines determine the time when the ratio c/c_0 was reduced to 1/e=0.37 (corresponding to a t=4h of treatment).

Figure 6. Ratio of the particle volume concentration (c/c_0) versus the mean Couette flow velocity ($\langle v_{Couette} \rangle$, in cm s^{-1}) for the runs with and without *D. magna* individuals.

Figure 7. Filtration capacity of *D. magna* individuals (in ml ind^{-1} h^{-1}) versus the mean Couette flow velocity ($\langle v_{Couette} \rangle$, in cm s^{-1}). Vertical dashed lines correspond to the different Couette flow regimes (Table 1). The horizontal line corresponds to the *D. magna* filtration in quiescent flow.

Figure 8. (a) F (in ml ind^{-1} h^{-1}) versus G (in s^{-1}) for the laminar-dominated flow regime. The dashed line represents the linear best fit of the data with an equation F=0.820G+0.767, with r^2=0.9797 and 99% confidence. **(b)** F (in ml ind^{-1} h^{-1}) versus G (in s^{-1}) predicted by the model (Equation (15)) for four different *D. magna* lengths (L=1 mm, 1.5 mm, 2 mm and 3 mm) in the laminar-dominated flow regime.